JOURNAL OF GEOPHYSICAL RESEARCH, VOL. 113, A04213, doi:10.1029/2007JA012537, 2008

Relation of substorm onset to Harang discontinuity

James M. Weygand,[1] R. L. McPherron,[1] H. U. Frey,[2] O. Amm,[3] K. Kauristie,[3] A. Viljanen,[3] and A. Koistinen[3]

Received 12 May 2007; revised 7 January 2008; accepted 30 January 2008; published 12 April 2008.

[1] In this study we investigate the relation of auroral substorm onset to the Harang discontinuity (HD). Various studies have reported that the substorm onset occurs poleward, equatorward, or within the HD. The motivation for the present study is to further investigate this relation with a much larger database. Using a database of over 3700 onsets determined from auroral images taken on the IMAGE spacecraft, we statistically examine the magnetic latitude location of the onset with respect to the location of the HD. The location of the discontinuity is determined with data from the IMAGE ground magnetometer network. We define the location of the HD as the transition from relatively strong eastward to relatively strong westward equivalent ionospheric currents at the latitude of the main nightside auroral electrojet flow. Our results show that the location of 75 onsets that occurred above the IMAGE ground array about 31% occurred within 6° of latitude of the HD observed during the growth phase of the substorm and 37% occur within 5° of latitude of the HD observed during the expansion phase. We also find that 23% of the onsets occur in association with vortices of ionospheric currents observed during the growth phase. The remaining 31% of the onsets do not appear to be associated with a HD or a vortex during the growth phase. Ten of the initial 75 onsets were identified as likely pseudo breakups and not fully developed substorms. Seven of the initial 75 onsets were probably poleward boundary intensifications (PBI). This study demonstrates that approximately 2/3 of the auroral substorm onsets do not occur within or near the HD identified in the growth phase. These results do not support the prediction made by Lyons et al. (2003) that substorm auroral onset should occur within the upward field aligned current in the Harang discontinuity.

Citation: Weygand, J. M., R. L. McPherron, H. Frey, O. Amm, K. Kauristie, A. T. Viljanen, and A. Koistinen (2008), Relation of substorm onset to Harang discontinuity, *J. Geophys. Res.*, *113*, A04213, doi:10.1029/2007JA012537.

1. Introduction

[2] The onset of the auroral substorm generally occurs in a region just before midnight at the boundary between the diffuse and discrete aurora. Normally, the most equatorward discrete arc intensifies and then expands both poleward and azimuthally [*Akasofu*, 1964]. Within the same region the complex feature of electrodynamics called the Harang discontinuity (HD) [*Heppner*, 1972] is also commonly observed. It was first described by *Harang* [1946] who characterized it as a region in the auroral oval near midnight slightly tilted north of west and across which the direction of magnetic perturbations observed by a single ground magnetometer switches from north to south. This is the boundary between the eastward and westward auroral electrojets. One of the initial difficulties in characterizing the HD was the paucity of ground magnetometers in the auroral region. With only a small number of magnetometers one can mix the spatial changes of the HD region with temporal changes such as those associated with the sudden enhancement of the westward electrojet during substorms. This problem can be circumvented with a large number of densely packed magnetometers spread in longitude and latitude. Figure 1 displays this change in direction of the eastward and westward auroral electrojet (solid green diagonal segment labeled classical HD). Figure 1 is similar to one shown as Figure 7 in *Koskinen and Pulkkinen* [1995]. Figure 1 also shows a reversal in the direction of the westward ionospheric current (dashed green segment) in the upper left of the figure, which is labeled the premidnight shear zone, and the upper right of the figure (black segment), which is labeled the postmidnight shear zone. These reversals in the current are not the classical HD referred to in the work of *Harang* [1946] because the change in the current direction occurs at the poleward boundary of the auroral oval and not within the oval. We emphasize that we do not consider the premidnight and postmidnight shears to be a part of the Harang discontinuity and that the premid-

[1]Institute of Geophysics and Planetary Physics, University of California, Los Angeles, California, USA.
[2]Space Physics Program, Finnish Meteorological Institute, Helsinki, Finland.
[3]Space Sciences Laboratory, University of California, Berkeley, California, USA.

0148-0227/08/2007JA012537$09.00

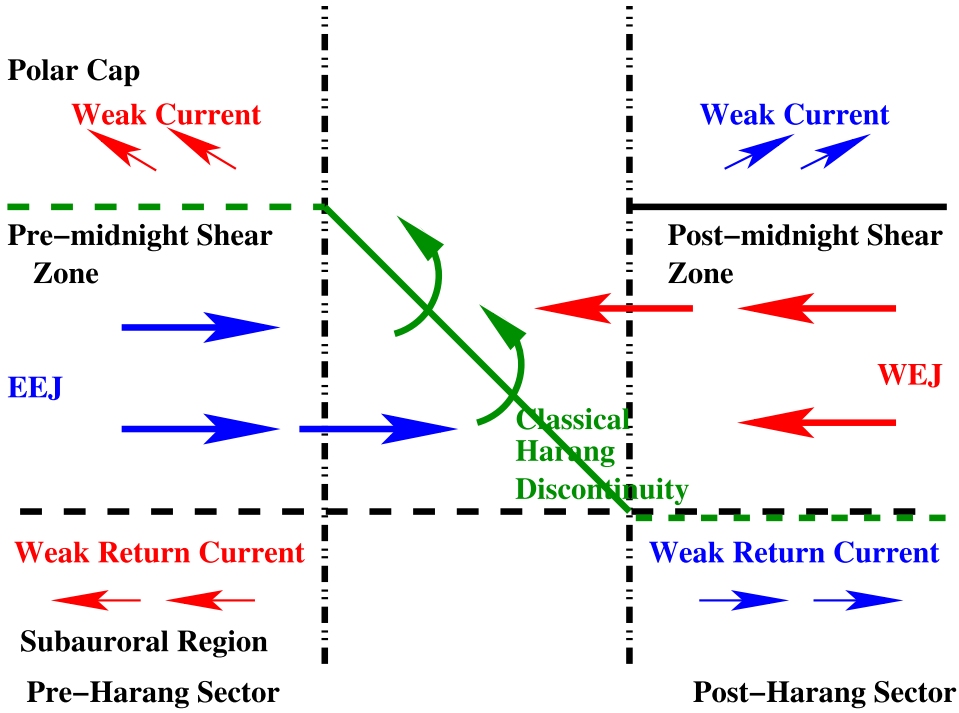

Figure 1. Idealized schematic of the Hall currents in the region of the Harang discontinuity. The blue arrows indicate the eastward electrojet, the red arrows represent the westward electrojet, and the solid green bar is the classical Harang discontinuity. To the west is the premidnight shear zone, which may not be connected to the Harang discontinuity, and to the east is the postmidnight shear zone.

night shear may not even be connected to the Harang discontinuity.

[3] The HD is formed in the ionosphere by the convection of magnetic field lines through the ionosphere. Open magnetic field lines convect antisunward from the dayside to the nightside across the polar cap and eventually are swept back into the magnetotail where they reconnect into closed magnetic field lines. After the field lines have closed, the ionospheric feet of these field lines reverse direction from antisunward to sunward in the midnight sector. The reversal of the flow from antisunward to sunward in the ionosphere does not form a true mathematical discontinuity as the name HD suggests and it is actually a few degrees wide as discussed by *Kamide* [1978]. The ionospheric electric fields in the HD sector converge in the region where the flow changes direction due to $\mathbf{E} = -\mathbf{v} \times \mathbf{B}$. Eastward and westward electrojets also converge near the HD and field-aligned currents (FACs) flow out of the ionosphere into the magnetotail. It is generally believed that the ionospheric HD couples with a shear in the convective flow in the premidnight sector of the magnetotail [*Maynard*, 1974; *Fairfield and Mead*, 1975; *Heppner*, 1977].

[4] However, a difference in latitude between the HD determined with ground magnetometers and the HD determined with radar data is commonly observed. *Kamide and Vickrey* [1983] reported that the location of the HD determined with ground magnetometers is equatorward of the location of the radar determined HD by about 1° to 2°. They suggest this is most likely due to differences in the strength of the eastward and westward electrojets. Typically, the westward electrojet is stronger than the eastward electrojet; thus the latitude at which the H-component reverses from a positive perturbation to a negative perturbation is a few degrees further equatorward [*Kamide and Vickrey*, 1983]. A similar observation of an approximate 2° to 3° difference between an equatorward HD identified with ground magnetometers and a poleward HD observed with the STARE radar data was described in a case study by *Kunkel et al.* [1986]. Kunkel et al. showed that at the location of the magnetic HD there was a FAC up out of the ionosphere and also showed that the Hall conductances peaked equatorward of the HD. *Amm* [2003] has also observed a latitudinal difference between the two definitions of the HD. They found the magnetic convection reversal boundary was 0.5–1.5° poleward of the electric convection reversal boundary in the postmidnight sector. They explain this difference as a consequence of the positive gradient of the absolute value of the field aligned current in the postmidnight sector.

[5] The upward FAC in the HD is also the location of the outward FAC in the substorm current wedge. The substorm current wedge forms during the expansion phase of the auroral substorm. It consists of a downward current in the morning sector, a westward current within the auroral bulge, and an outward current from the westward surge. *Lyons et al.* [2003] believe that the substorm current wedge and the auroral onset are both consequences of a reduction in the strength of magnetospheric convection that leads to a divergence of plasma sheet particles by diamagnetic drift. They claim that the upward current in the substorm current

wedge is due to westward gradient/curvature drift of $\mathbf{E} \times \mathbf{B}$ convecting plasma in the plasma sheet [*Erickson et al.*, 1991]. According to *Erickson et al.* [1991], the dawn flank of the tail does not have a source of energetic ions and the westward gradient/curvature drift of $\mathbf{E} \times \mathbf{B}$ convecting plasma results in the depletion of energetic ions in the dawn sector of the plasma sheet. This dawnside depletion means that on average, the duskside of the plasma sheet will have higher ion temperatures, pressures, and flux tube content and hence stronger westward cross-tail drift current than the dawnside. As a result, the cross-tail divergence of drift current finds closure through the FACs connecting the tail currents to the HD (i.e., auroral onset location) in the ionosphere.

[6] Several studies have investigated the relation of the location of substorm onset to the HD. *Nielsen and Greenwald* [1979] found it is typically located poleward of or colocated with the HD as determined from magnetic field observations. In contrast, *Baumjohann et al.* [1981]; *Koskinen and Pulkkinen* [1995] used radar observations to show the onset is located equatorward or colocated with the HD. This lack of agreement demonstrates that the location of the substorm onset relative to the HD is not yet clear. The motivation of the work reported here is to determine which of these reports is correct. As we will demonstrate, our results support most of the previous studies and it is the method used to locate the HD that causes confusion.

[7] While substorm onsets have been frequently associated with the HD, a number of studies have also shown that the substorm occurs near a vortex in the equivalent ionospheric currents [*Untiedt et al.*, 1978; *Küppers et al.*, 1979; *Opgenoorth et al.*, 1980; *André and Baumjohann*, 1982; *Untiedt and Baumjohann*, 1993; *Lyatsky et al.*, 2001]. *Küppers et al.* [1979] used equivalent ionospheric currents to demonstrate that the vortex in the currents was present after the substorm onset. *Untiedt et al.* [1978] used both the Finnish Meteorological Institute all-sky cameras and the equivalent ionospheric currents (see section 3.2) calculated from the ground magnetometer data to show for a single case that an equivalent ionospheric current vortex was present before the substorm onset. They also noted that preexisting auroral activity was present before the onset. In the work of *Opgenoorth et al.* [1980] a single event was examined in detail with an array of Scandinavian all-sky imagers and ground magnetometers and it was shown that an equivalent ionospheric current vortex formed at about the time of a substorm onset and was present for several minutes after the onset. *André and Baumjohann* [1982] examined near simultaneous electric field and magnetic field measurements in and around a vortex observed in the equivalent ionospheric current during a series of omega bands. They found that the electric field and currents were nearly perpendicular to one another and they concluded that the vortex loops around a FAC with little or no conductivity gradients in the ionosphere. A more recent study by *Lyatsky et al.* [2001] showed that a substorm identified with the Interball UV imager appeared near a vortex in the equivalent ionospheric currents [*Lyatsky et al.*, 2001]. Unfortunately, the Lyatsky et al. study did not have near simultaneous Interball UV images of the substorm auroral onset and the current vortex so a one to one correspondence between the onset location and vortex was not possible; however, they could conclude that the westward surge was collocated with a counter clockwise vortex.

2. Instrumentation

[8] Data from the Imager of Magnetopause-to-Aurora Global Exploration (IMAGE) spacecraft and the International Monitor for Auroral Geomagnetic Effects (IMAGE) ground magnetometer array are used in this study. Auroral images identifying substorm onsets were obtained by the IMAGE far ultraviolet (FUV) photon imagers. Ground magnetometer data from the IMAGE ground array were inverted providing maps of overhead equivalent ionospheric currents, which were then used to identify the HD and calculate the local *AL* index.

[9] The IMAGE spacecraft was launched in March of 2000 and put into an elliptical polar orbit with an apogee of 7.2 Earth radii (45,922 km) and a perigee of 1000 km [*Burch*, 2003]. The spacecraft carried six instruments. The FUV instrument had three photon imagers, the Wideband Imaging Camera (WIC) and two channels, SI-12 and SI-13, of the Spectrographic Imager (SI). The WIC and SI-13 imagers observed emissions from atmospheric neutrals that are excited by secondary electrons produced by both precipitating electrons and protons. The SI-12 imager was sensitive to the proton aurora hydrogen emissions [*Mende et al.*, 2003]. The three imagers observed the aurora for about 5 to 10 s per 2 min spin. Because FUV is mounted on a spinning spacecraft the pointing is continually corrected with bright UV stars within the field of view. However, the final pointing error in the spin plane can be up to 4 pixels and up to 2 pixels in the plane perpendicular to the spin plane.

[10] The IMAGE array consists of 29 ground magnetometers maintained by ten institutes from Estonia, Finland, Germany, Norway, Poland, Russia, and Sweden. The stations cover 58° to 79° geographic latitude, which is ideal for electrojet studies. At each station the magnetic field vector is sampled once every 10 s and all magnetometers have a nominal accuracy in the magnetic field of about ±0.1 nT for the permanent observatories. In addition to the instrumental accuracy there is a baseline uncertainty that varies from event to event.

[11] The IMAGE array of ground magnetometers is also used to construct the local *AL* indices that are employed in this study. The local *AE* indices were calculated with a procedure similar to the global *AE* indices. This procedure consists of automatically defining the baseline values for each month, which is the quietest 3 h interval in a day where "quiet" refers to the period with the smallest difference between the maximum and minimum H value. The H component of the stations are superposed after subtracting the baselines and the lower envelope of the curves is used to determine the *AL* indices while the upper envelope of the curves is used to calculate the *AU* indices [*Kauristie et al.*, 1996].

3. Procedure

3.1. Identifying the Substorm

[12] All of the substorm onsets used in this study were identified with the procedure described by *Frey et al.* [2004]

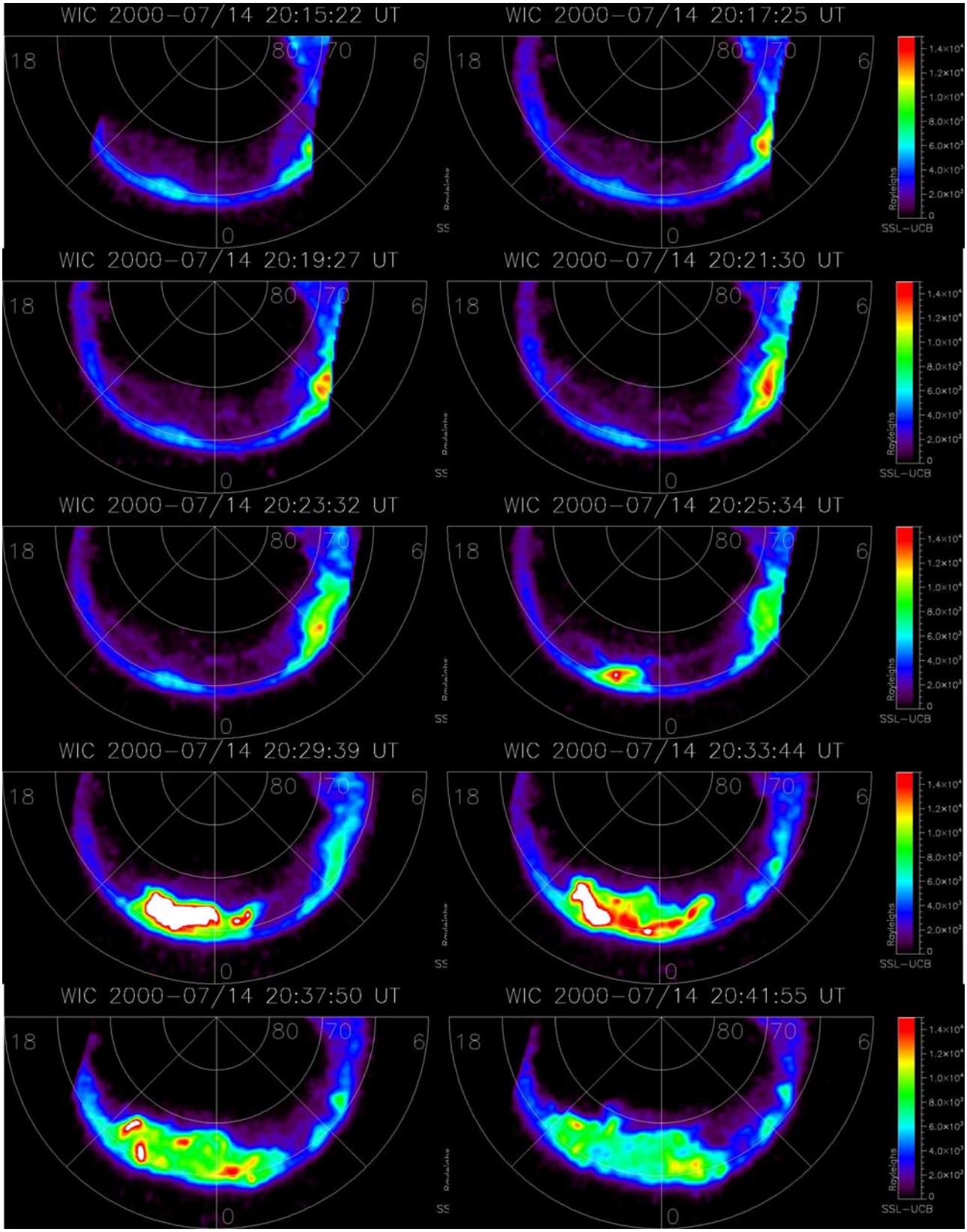

Figure 2. Sequence of processed IMAGE WIC auroral images of the 14 July 2000 substorm at 2023:32 UT. These images have been projected on a two dimensional plane tangent to the north magnetic pole.

and *Frey and Mende* [2006]. As discussed in these studies, most of the substorm onsets are identified with the WIC images because the spatial resolution of the WIC imager is better than the SI-12 and SI-13 imagers. When WIC images did not provide the ideal view of the auroral oval the SI-13 images were used instead. The onsets in this study meet the following criteria: (1) there was a clear local brightening of the aurora and the center of the brightening is taken as the location of the onset, (2) the aurora had to expand poleward in the auroral oval and spread azimuthally in local time for at least 20 min, and (3) 30 min had to pass between substorms onsets to be consider separate events. Figure 2 displays a good example of a substorm onset at 2023:32 UT on 14 July 2000 that meets these criteria. The purpose of criteria 2 and 3 is to eliminate pseudo-breakups, poleward boundary intensifications (PBIs), and multionset substorms from our study. Approximately 3700 substorms observed in the northern auroral oval satisfy these criteria. As an additional means of verifying the substorm onset identification we examined the local *AL* index for a sharp decrease of at least −50 nT followed by a gradual recovery.

3.2. Identifying the Harang Discontinuity

[13] The HD is identified from the equivalent ionospheric currents derived with a matrix inversion technique that uses the measured ground magnetic disturbance in the IMAGE ground array [*Amm*, 1997, 1998; *Amm and Viljanen*, 1999; *Amm et al.*, 2000]. The Amm and Viljanen technique defines two elementary current systems. The first is a divergence-free current system flowing parallel to the Earth's surface and representing the mainly ionospheric Hall current but only if the model ionospheric conductances happen to be uniform, which is unlikely during substorms. The second is a curl-free current system that represents both the FACs and the Pedersen currents. The superposition of these two current systems can reproduce any vector field on a sphere. If it is known a priori that the vector field is curl-free or divergence-free only one set of basic functions is needed, and thus 50% of the free coefficients associated with the other current system can be removed. In this study we only determine the divergence-free currents. Since our study employs data from only the IMAGE ground array the basis functions are local, and thus the density and geometry of elementary current systems to be determined can be adjusted according to the density and geometry of the ground magnetometer data. No fixed upper and lower wavelength needs to be specified for the modeling, as is needed in harmonic expansions and no boundary conditions are required. Careful testing of this method has already been done by *Pulkkinen et al.* [2003]. Their results were validated by means of synthetic ionospheric current models and by investigating the goodness of fit between modeled and measured ground magnetic field. They found that errors on the order of 1% occur when the equivalent ionospheric currents are determined in the region of the ground magnetometers, but farther from the ground magnetometers the error typically increase to 15%.

[14] With the derived equivalent ionospheric currents over the IMAGE array we then attempt to qualitatively identify (i.e., visual examination) the HD as a region between *strong* westward and eastward currents where $J_y = 0$ in geographic coordinates, as is defined by *Maynard* [1974] and *Heppner* [1977] at the latitude of the nightside auroral oval. Figure 1 displays an idealized picture of the Hall currents in the vicinity of the HD. The classical HD is identified with the solid green segment. Figure 1 also displays two other shears at the location of the dashed green segments between the eastward electrojet and the weak poleward ionospheric currents and between the westward electrojet and the weak equatorward ionospheric return currents. For this study we do not consider these shears to be part of the HD defined by *Maynard* [1974] and *Heppner* [1977]. As we will see, in many cases the orientation of the HD is clear when the IMAGE array is located in the premidnight sector. However, in just as many cases the HD is not located near the IMAGE array.

3.3. Identifying Equivalent Ionospheric Current Vortices

[15] A significant fraction of the onsets in our study display a current pattern that has previously been described as a vortex [*Untiedt et al.*, 1978; *Opgenoorth et al.*, 1980; *Lyatsky et al.*, 2001]. The vortex appears as a rotation in the equivalent ionospheric currents. To be identified as a vortex, we require that the equivalent ionospheric currents rotate about an axis on all sides. This definition allows us to eliminate the HD that sometimes shows a rotation from an eastward to westward electrojet as shown in Figure 1. In this study we observe two different vortices: those with a clockwise rotation and those with a counter clockwise rotation, which indicate the presence of an upward FAC and downward FAC, respectively [*Untiedt et al.*, 1978; *Opgenoorth et al.*, 1980].

3.4. Simultaneous Observations of the Onset and the Harang Discontinuity

[16] With the database of substorms onsets we searched for events that occurred within 6° longitude of the central line of the IMAGE magnetometer array from about Ny Ålesund (NAL) to Oulujärvi (OUJ). The choice of a range of 6° is arbitrary. Of the approximately 3700 substorms onsets available, 75 were observed within 6°. With this subset the equivalent ionospheric currents are derived using the near simultaneous IMAGE array measurements (i.e., observations made within 10 s of the auroral onset) and then visually examined for evidence of a HD. The HD is defined as the region between strong westward currents on the poleward side of the auroral oval and strong eastward currents on the equatorward side. The top of Figure 3 shows a reversal in the current system characteristic of the HD. Once the HD is defined we measure the latitudinal difference in a meridian between an extension of the HD and the onset location.

[17] To quantify the relation of the auroral onset to the HD, we measure the difference in latitude between the HD in the substorm growth phase determined from the local *AL* index and the auroral onset location just after the expansion onset. We use the preonset HD for reference because once the substorm has begun the ionospheric currents can become complicated and do not necessarily reflect the position of the HD at the time of onset. On average the substorm onset in the *AL* index occurs about 4 min before the auroral image onset; however, this difference is sometimes as large as 10 min and sometimes nearly zero.

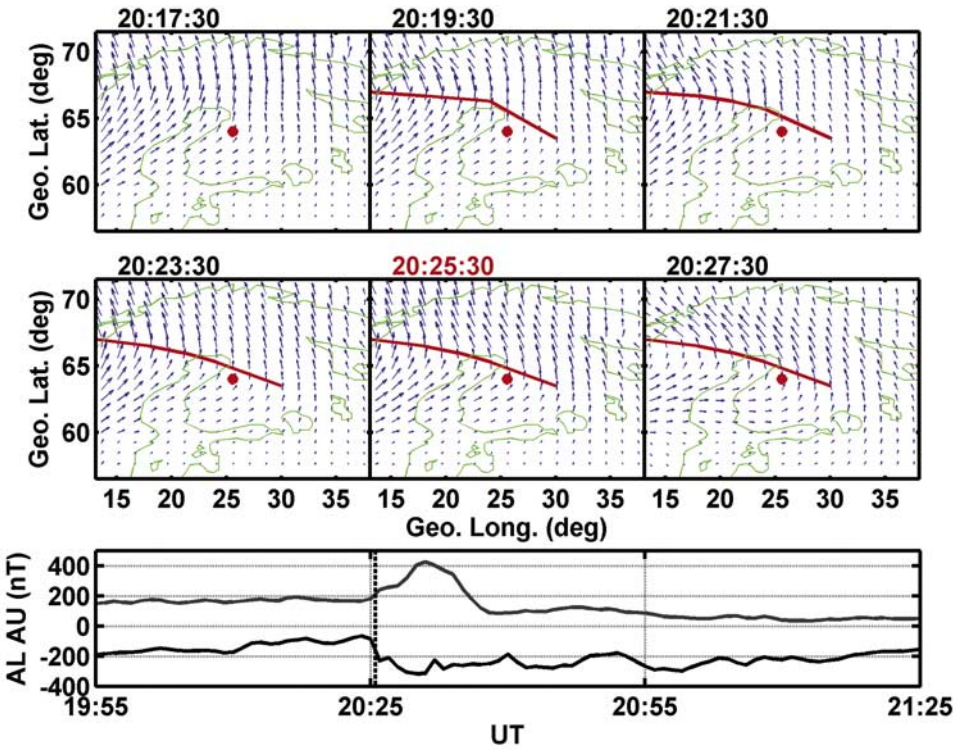

Figure 3. The top six panels are the equivalent ionospheric currents (blue vectors), plotted over the Scandinavian region (green outline) and the estimated HD location (red curve). Note that the size of each panel is 15° by 25°. The substorm onset position is given in every panel with the red asterisk at 64.0° geographic latitude and 25.6° geographic longitude. At the top of each image is the UT time (black) and the auroral onset time (red). The lower panel shows the local *AU* and *AL* indices. The substorm onset time observed in the auroral images is indicated by the vertical horizontal dashed line.

[18] The longitudinal distance between the HD and auroral onset is not determined because the orientation of the HD is often nearly parallel to the lines of longitude. Since the orientation of the HD is qualitatively defined we estimate the uncertainty in the measured difference is on the order of 1° in latitude.

[19] The 75 onsets can be classified into five categories: (1) onsets that are not associated with a local *AL* decrease, (2) onsets in the poleward portion of the auroral oval that have an accompanying decrease of at least −50 nT in local *AL* within 10 min of the IMAGE spacecraft identified onset, (3) onsets in the equatorward portion of the auroral oval that have an accompanying decrease of at least −50 nT in local *AL* within 10 min of the IMAGE spacecraft onset observation and are associated with a HD in the simultaneous equivalent ionospheric currents, (4) onsets in the equatorward portion of the auroral oval that show a decrease of at least −50 nT in the local *AL* within 10 min of the IMAGE spacecraft observations and are associated with a nearly simultaneous vortex in equivalent ionospheric currents, and (5) onsets in the equatorward portion of the auroral oval that show a decrease in *AL* and no near simultaneous HD or equivalent ionospheric current vortex.

4. Observations

[20] Each of the 75 substorm onsets has IMAGE ground magnetometer data that were used to obtained equivalent ionospheric currents. In the next five sections we will discuss the five different categories.

4.1. Onset Without Negative Bay in *AL* and No Harang Discontinuity

[21] Ten of the 75 sudden auroral brightenings do not show a sudden decrease in the IMAGE *AL* index as would be expected for a substorm event. We will refer to these events as ''onsets'' in order to differentiate them from auroral substorm onsets. This fraction of ''onsets'' without a sharp drop in *AL* is larger if we use the World Data Center *AL* index instead of the local *AL* determined by the IMAGE ground array. Closer inspection of the auroral image data shows that about six of these ''onsets'' exhibit very little expansion of the auroral bulge. Three onsets display moderate expansion. One of the ''onsets'' on 17 October 2001 at about 1920 UT shows a significant expansion of the auroral bulge about 6 min after the initial brightening, but only a small change in *AL* is present and the change occurs 15 min after the brightening. There is, however, a sharp change of about 10 nT in *AL* about 15 min before the onset. For this study a sharp decrease in the local *AL* index is required to be considered a substorm onset and for the remainder of this study these events will be treated as pseudo breakups. The pseudo breakups will not be considered in the statistics of the HD and the auroral onset location, but they will be discussed separately.

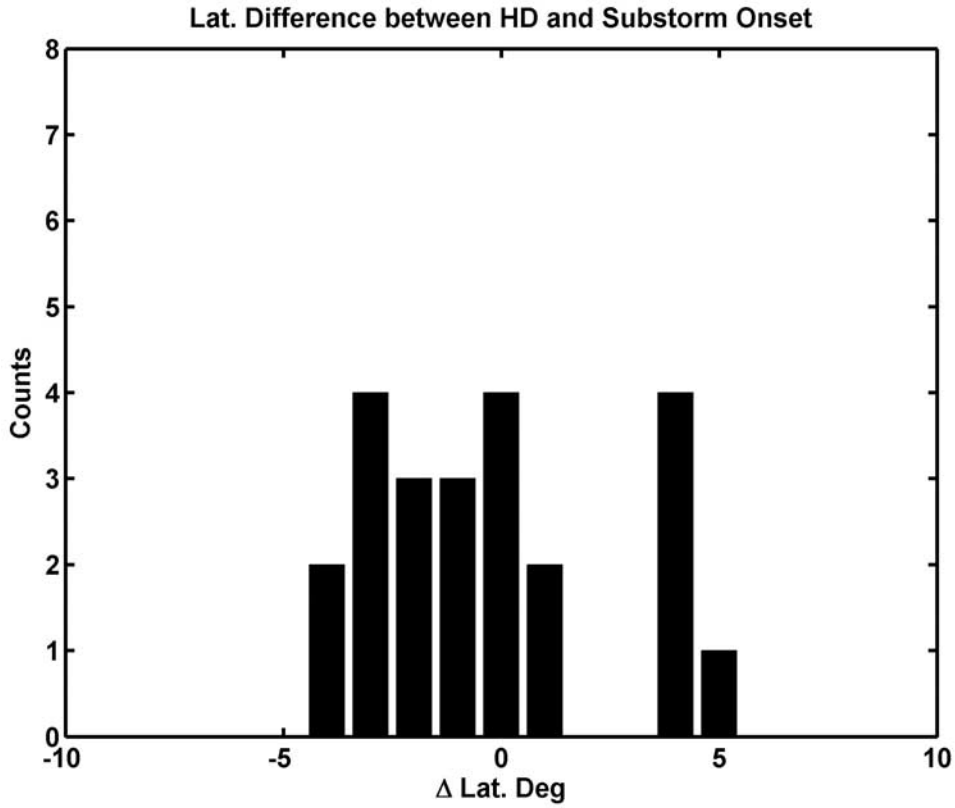

Figure 4. Histogram of the difference in latitude between the substorm onset and HD during the growth phase. Negative values indicate that the HD is equatorward of the onset position.

4.2. PBI Onsets With Negative Bay in *AL*

[22] Seven of the 75 sudden auroral brightenings occur at the approximate poleward edge of the auroral oval. LANL/SOPA data near the meridian of the IMAGE array is available for five of the events and no ion or electron injection is apparent as is usually associated with substorms. Furthermore, the midlatitude ground magnetometers displayed little or no Pi2 pulsation activity as we would expect during a substorm. We will refer to these events as PBIs in order to differentiate them from auroral substorm onsets. However, all of these events displayed a sharp decrease in the local *AL* index. Closer inspection of the auroral image data shows that all of these PBIs exhibit some expansion poleward of the auroral oval and the bulk of the expansion develops equatorward from the onset. In all these events the sudden brightening associated with the onset spread azimuthally along the auroral oval. The PBIs will not be considered in the statistics of the HD and the auroral onset location, but they will be separately discussed.

4.3. Substorm Onsets With Negative Bay in *AL* and a Harang Discontinuity

[23] Of the 75 onsets near the IMAGE array, 23 onsets show a sharp decrease in the local *AL* index with a change of at least −50 nT and the equivalent ionospheric currents indicate that a HD was present during the growth phase. Thirty-three onsets occurred near a HD observed during the expansion phase. However, only 18 HDs are continuously present during the growth phase and into the expansion phase. Five of the HDs during the growth phase either disappeared about the time of onset and reappeared or disappeared all together. During the expansion phase a number of the HDs formed or move into the array of equivalent ionospheric currents. Figures 2 and 3 are examples of the ideal case for this category of onsets. Figure 2 displays a sequence of auroral images from the IMAGE spacecraft illustrating a substorm expansion. The auroral onset is at 2023:32 UT on 14 July 2000 and is followed by the expansion phase and recovery phase. Figure 3 displays both the equivalent ionospheric currents in a geographic coordinate system as calculated by *Amm and Viljanen* [1999] and the locally determined *AL* index. The top six panels present the equivalent ionospheric currents for six different times as indicated above each panel. The HD is denoted by a thick bar and the onset location is indicated with the asterisk at 64.0° geographic latitude and 25.6° geographic longitude. The uncertainty of the onset location is approximately 1° and these error bars are approximately the size of the asterisk. In this event the onset appears to take place in an eastward current system. Figure 3 (bottom) shows the sharp decrease in the local *AL* index. The onset time identified in the image is indicated with a vertical dashed line.

[24] Not all 28 HD events are as obvious as the one in Figure 3; however, in all cases the orientation of the HD is well determined and the difference in latitude between the onset and the HD can be measured. Figure 4 (growth phase HDs) and Figure 5 (expansion phase HDs) present the

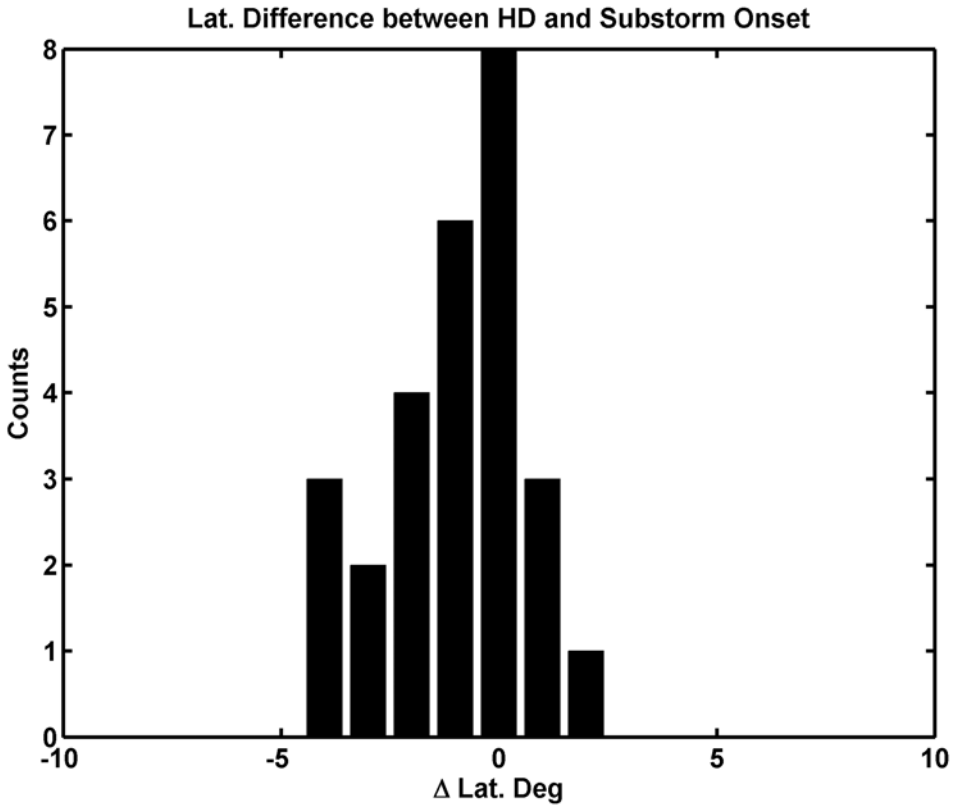

Figure 5. Histogram of the difference in latitude between the substorm onset and HD during the expansion phase. Negative values indicate that the HD is equatorward of the onset position.

distribution of measured latitudinal differences with negative values of Δlat indicating that the HD is equatorward of the location of the initial auroral brightening. During the growth phase, the mean Δlat is $-0.53°$, the median is about $-0.8°$, and the standard deviation is 2.7°. During the expansion phase, the mean Δlat is $-1.0°$, the median is about $-1.0°$, and the standard deviation is 1.5°. Table 1 indicates the number of events that went into the distributions.

[25] In addition to measuring Δlat we also determined the direction of the electrojet current associated with the onset location. Table 1 lists the number of events with an equivalent ionospheric current westward electrojet (EIC WEJ), eastward electrojet (EIC EEJ), and those colocated with the HD at the location of the onset during both the growth and expansion phases of the substorm. During the growth phase 12 (52%) of the onsets occurred within the EIC WEJ, 0 occurred within the HD, 8 (35%) occurred within the EIC EEJ, and 3 onsets were unclear, which means the equivalent ionospheric current showed neither westward nor eastward current. During the expansion phase, 23 (85%) of the onsets occurred within the EIC WEJ, 2 (9%) occurred within the discontinuity, and 2 occurred within the EIC EEJ. Those onsets that occurred within the EIC EEJ were within 3° of the HD.

Table 1. Categorization of the Auroral Onset Events During the Expansion Phase and the Growth Phase of the Substorm[a]

	No *AL* Decrease	HD	Vortex	Both HD and Vortex	Neither
Growth phase	10	23 (18)	17	5	23
	WEJ: 5	WEJ: 12	WEJ: 16	WEJ: 5	WEJ: 17
	EEJ: 4	EEJ: 8	EEJ: 1	EEJ: 0	EEJ: 5
	HD: 0	HD: 0	HD: 0	HD: 0	HD: 0
	unclear: 1	unclear: 3	unclear: 0	unclear: 0	unclear: 1
Expansion phase	10	28 (18)	37	20	13
	WEJ: 5	WEJ: 23	WEJ: 33	WEJ: 17	WEJ: 11
	EEJ: 4	EEJ: 2	EEJ: 1	EEJ: 1	EEJ: 0
	HD: 0	HD: 3	HD: 3	HD: 2	HD: 0
	unclear: 1	unclear: 0	unclear: 0	unclear: 0	unclear: 2

[a]Events with no local *AL* decrease are consider to be pseudo-breakups and do not differ during the growth phase and expansion phase. The second value in parenthesis in the HD category indicates the number of continuous HDs throughout both the growth and the expansion phase.

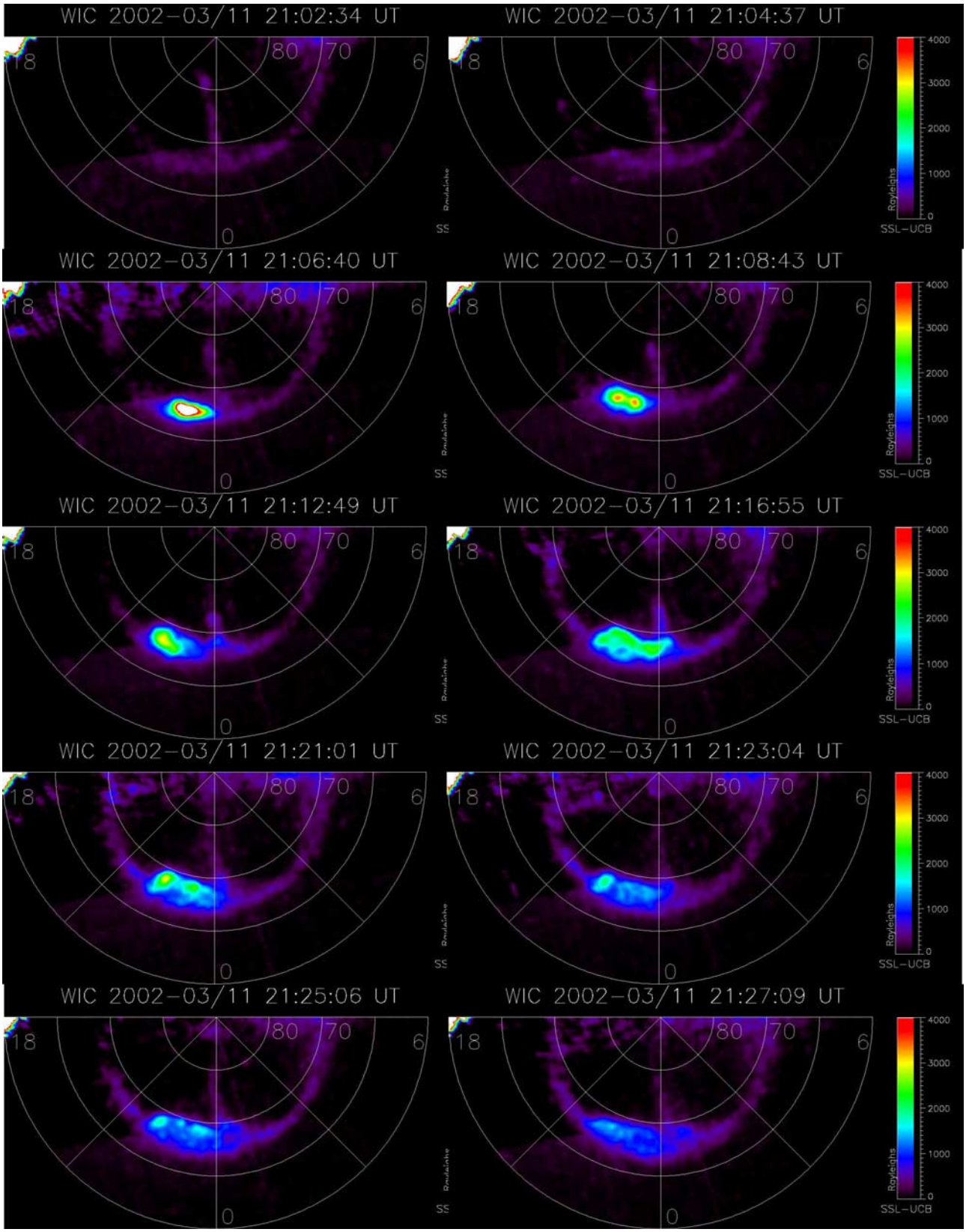

Figure 6. Sequence of processed IMAGE WIC auroral images of the 11 March 2002 substorm at 2106:40 UT. These images have been flattened to a two dimensional plain tangent to the north magnetic pole. This figure has the same format as Figure 2.

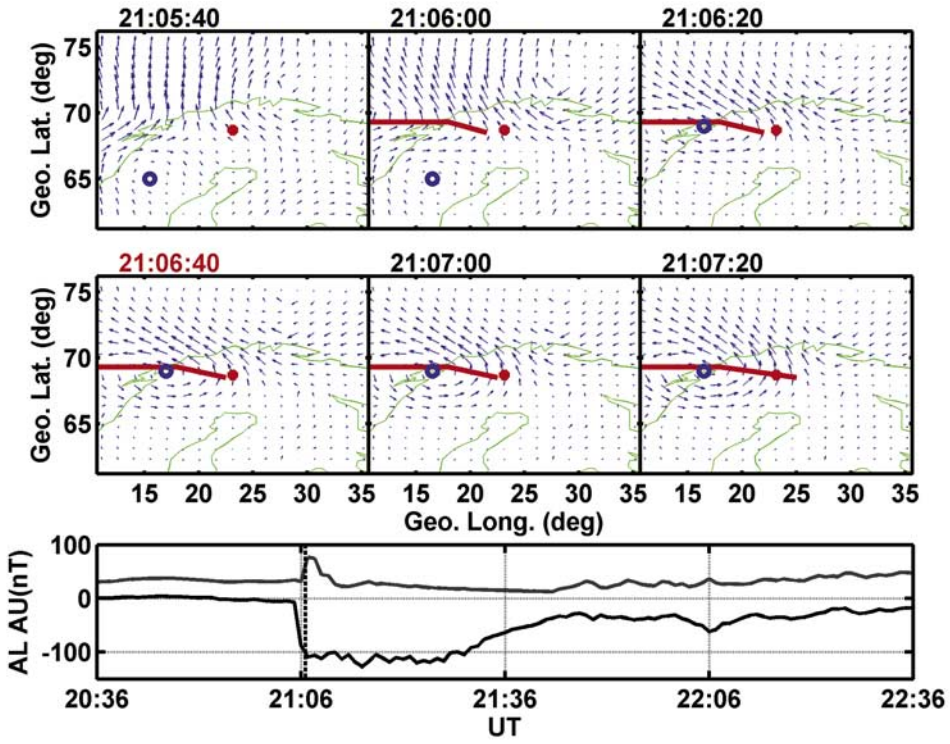

Figure 7. In the upper six panels are the calculated equivalent ionospheric currents. This figure has the same format as Figure 3. The substorm onset position is given with the red asterisk at 68.7° geographic latitude and 23.1° geographic longitude and the center of the equivalent ionospheric current vortex is indicated with the blue circle. In the lower panel is shown the local *AU* and *AL* indices.

4.4. Substorm Onsets With Negative Bay in *AL* and a Vortex

[26] Of the 75 onsets 17 had an equivalent ionospheric current vortex present during the growth phase and 37 had an equivalent ionospheric current vortex present at the time of the auroral onset. Figure 6 and Figure 7 present a sequence of auroral images and equivalent ionospheric currents representing this category of onsets. The onset began at 2106:40 UT on 11 March 2002 and was followed by the expansion and recovery phases. The center of the equivalent ionospheric current vortex was located near geographic latitude and longitude of (68.7°, 23.1°). A HD is also evident in the maps of equivalent current. During several of the onsets both a vortex and a HD were present. Table 1 indicates the number of cases during the growth and expansion phase displaying vortices in the equivalent ionospheric current and those with both an equivalent ionospheric current vortex and HD.

[27] As with the HD we have measured the latitudinal separation between the center of the equivalent ionospheric current vortex and the auroral onset location. Figure 8 and Figure 9 are distributions of the Δlat separations during the growth and expansion phase. During the growth phase the mean Δlat separation is −0.1°, the median is −1.2°, and standard deviation is 3.4°. During the expansion phase the mean Δlat separation is −0.2°, the median is −0.4°, and standard deviation is 2.4°. With the equivalent ionospheric current vortices we are also able to measure the longitudinal separation. These distributions are given in Figures 10 and 11 where negative values of Δlong indicate the vortex is to the west of the auroral onset and positive values indicate it is east. During the growth phase the mean Δlong separation is 1.3°, the median is 0.0°, and the standard deviation is 6.1°. During the expansion phase the mean Δlong separation is 0.8°, the median is 0.7°, and the standard deviation is 5.4°.

[28] As we found for the HD category, the bulk of the onsets near equivalent ionospheric current vortices also occur within the EIC WEJ. Sixteen onsets are associated with the EIC WEJ and one occurred within the EIC EEJ during the growth phase. During the expansion phase 33 onsets were associated with the EIC WEJ and one occurred within the EIC EEJ. None of the onsets occur within the HD during the growth phase. During the expansion phase 3 of the onsets occurred within the HD. The number of onsets for each equivalent ionospheric current type is given in Table 1.

4.5. Substorm Onsets With Negative Bay in *AL* and No Harang Discontinuity or Vortex

[29] Of the 75 events, 23 (31%) display a decrease in *AL*, but had no clear HD or vortex in the growth phase and 13 (17%) had neither during the expansion phase. This could be related to the limited area covered by the ground magnetometer array; however, the choice of a 6° longitudinal difference between the substorm onset and the central line of the ground magnetometers was chosen to help accurately identify the equivalent ionospheric current pat-

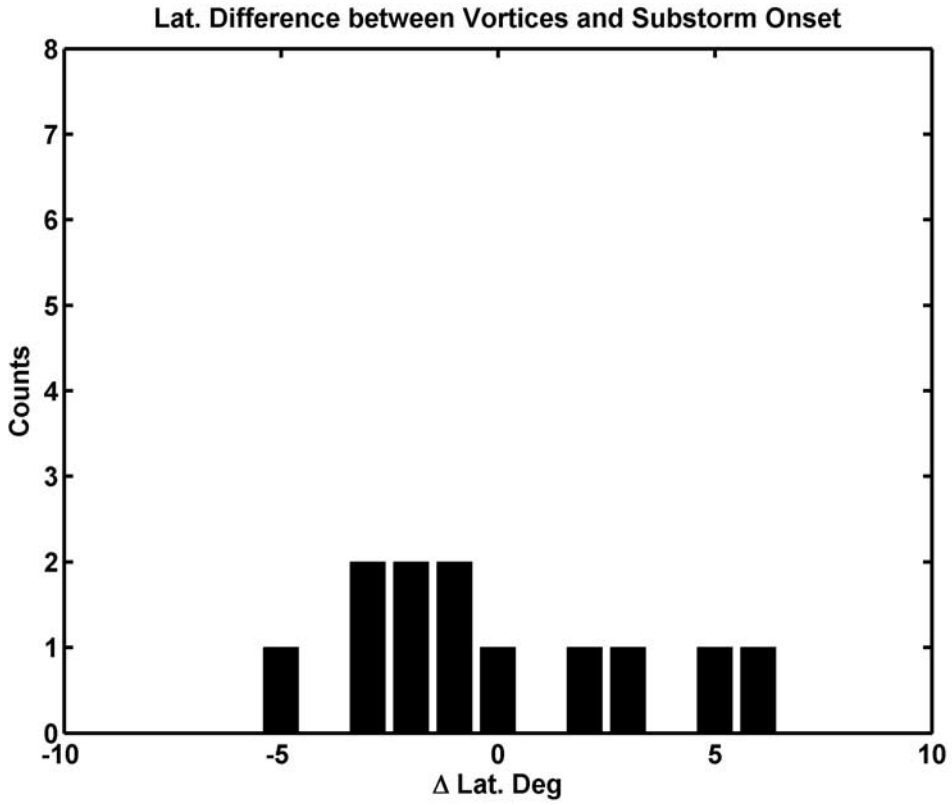

Figure 8. Histogram of the difference in latitude between the substorm onset and the equivalent ionospheric current vortex during the growth phase. Negative values indicate that the vortex is equatorward of the onset position.

tern associated with the substorm onset. We discuss this topic in greater detail in a later section.

[30] Using the simple diagram given in Figure 1 we are able to determine that 7 of the 23 events occurred during the growth phase in the region labeled as the post-Harang sector. During the expansion phase 5 of the 13 events occurred in the region labeled as the post-Harang sector. This region is identified by the strong EIC WEJ and the considerably weaker eastward EICs poleward and equatorward of the EIC WEJ. Some researchers might identify this shear in the equivalent ionospheric currents as a HD, but we do not because it is not the classical definition referred to by *Harang* [1946]. Two onsets also occurred in the region labeled as the pre-Harang sector during the growth phase and none during the expansion phase. This sector is identified by the strong EIC EEJ and the considerably weaker westward EICs poleward and equatorward of the EEJ shown.

[31] For this category of onsets without HDs and vortices we could identify the electrojet direction for 23 events during the growth phase and 11 during the expansion phase. The bulk of the events occur within the EIC WEJ during both the growth and the expansion phase and a small portion of the onsets occur within the EIC EEJ during the growth and expansion phase. The distribution of the onsets for this category based on the equivalent ionospheric current direction is given in Table 1.

[32] Several of the onsets in this section can be placed in a subcategory that can be best described as almost entirely EIC WEJ or EIC EEJ. Eleven of the other auroral onsets occurred in regions of almost entirely EIC WEJ and two onsets occurred in regions of almost entirely EIC EEJ during the growth phase. Five of the other auroral onsets occurred in regions of almost entirely EIC WEJ and no onsets occurred in regions of almost entirely EIC EEJ during the expansion phase.

5. Discussion

[33] In this section we will discuss each of the different onset and equivalent ionospheric current categories.

5.1. Onset Without Negative Bay in *AL* and No Harang Discontinuity

[34] In this study we treated ''onsets'' that were not associated with a sharp decrease in *AL* as probable pseudo breakups. The auroral images are available for all 10 of these events and they display minimal expansion of the initial brightening in 6 out of 10 events while three display moderate expansion. Only one event on 17 October 2001 at about 1920 UT displayed a significant auroral bulge expansion of the initial brightening. The auroral emissions may have been too weak to detect prior to the brightening and the observed expansion is the result of enhanced emissions and not necessarily an expansion of the auroral bulge. The *AL* index for all ten events shows little or no change within a 20 min window centered on the onset even though the brightening occurred within a few degrees of a ground

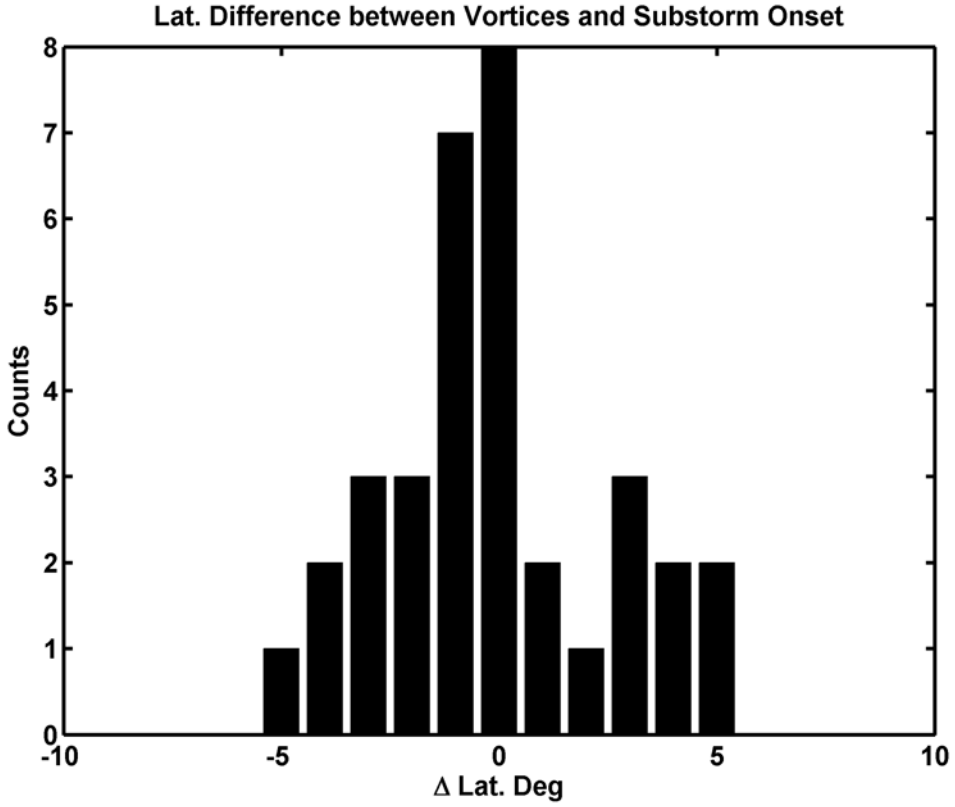

Figure 9. Histogram of the difference in latitude between the substorm onset and the equivalent ionospheric current vortex during the expansion phase. Negative values indicate that the vortex is equatorward of the onset position.

magnetometer station. The largest decrease observed in the local *AL* index for these 10 events was only 40 nT. Furthermore, LANL SOPA data from the approximate meridian of the IMAGE array is available for 9 of the 10 events. Three of the nine ''onsets'' show a simultaneous injection of particles that might be attributed to a substorm onset, but dispersionless injections have been associated with pseudo-breakups as well as full breakups [*Koskinen et al.*, 1993; *Nakamura et al.*, 1994; *Pulkkinen et al.*, 1998]. Unfortunately, there were no LANL/SOPA data available near the meridian of the IMAGE array for the 17 October 2001 event.

[35] Whether these ''onsets'' are pseudo-breakups is not obvious, but they clearly demonstrate that it is often difficult to decide between a pseudo-breakup and a substorm expansion. In the ideal substorm model there should be a sudden brightening somewhere in the auroral oval plus an expansion of the initial brightening, the westward electrojet should become enhanced, and geosynchronous spacecraft should see a simultaneous injection in the ions, electrons, or both. The fact that one or more of these phenomena are not present suggests that not all the ''onsets'' are substorms. It could be argued that the LANL spacecraft that saw no injections was not ideally located to observe an injection. However, we do not rely on the LANL/SOPA data to identify substorm expansions and these observations merely support the identification of the substorm onsets. The lack of a clear enhancement in the local *AL* index is puzzling if the aurora always follows the pattern expected for an ideal auroral substorm. It is possible in some cases that the ground magnetometer array was not ideally located to observe the westward electrojet enhancement and this might be the case for 7 of the 10 events that seem to be located in the pre-Harang sector. This observation would mean that the location of these ''onsets,'' if they are substorms was far from the HD and EIC WEJ, which would contradict previous studies. However, more information is required to support this statement. Three of the 10 events were observed in a significant EIC WEJ. The lack of a significant change in the EIC WEJ for these three ''onset'' supports the conclusion that these events were pseudo breakups. We note that one of these three ''onsets'' was observed at nearly the same time as a simultaneous injection in the LANL/SOPA data. Again, this is not surprising since a number of studies have observed dispersionless injection associated with pseudo-breakups [*Koskinen et al.*, 1993; *Nakamura et al.*, 1994; *Pulkkinen et al.*, 1998]. If that one event is then a pseudo-breakup but *Frey et al.* [2004] and *Frey and Mende* [2006] observed a poleward and azimuthal expansion of the aurora, then we might interpret our observations as support for the idea that pseudo breakups are small-scale substorms with many of the same characteristics as substorms except with limited scale size and strength. The important point is that for these 10 events the observations are ambiguous and we do not include them in our statistics.

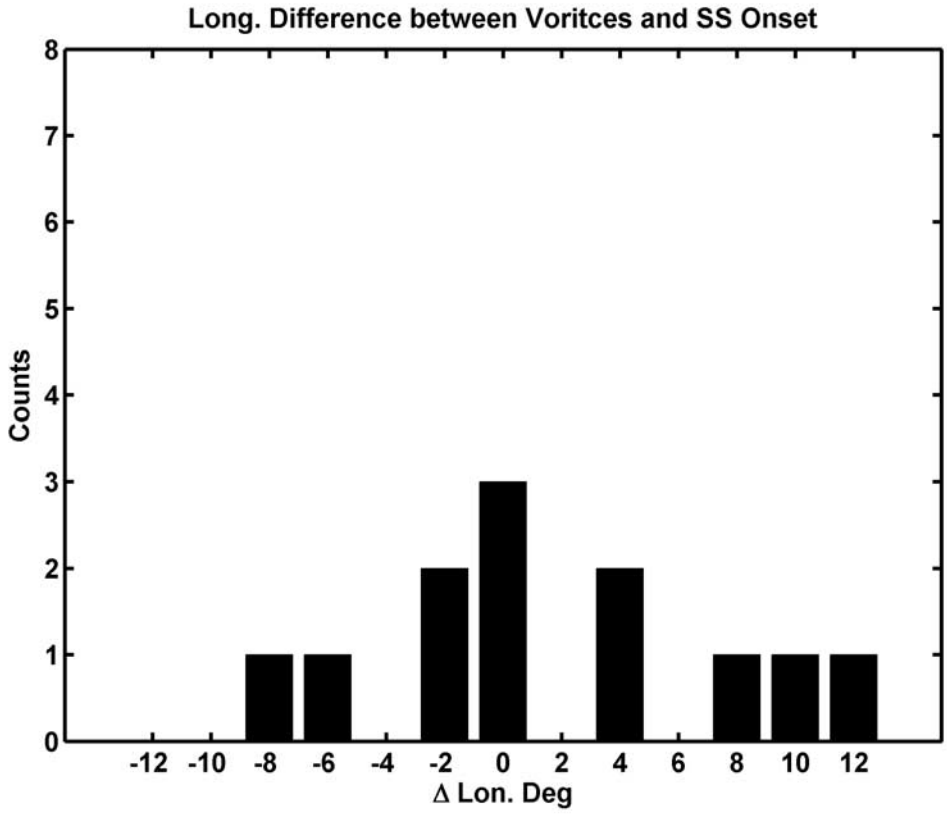

Figure 10. Histogram of the difference in longitude between the substorm onset and the equivalent ionospheric current vortex during the growth phase. Negative values indicate that the vortex is to the west of the onset position and positive values for vortices to the east.

5.2. PBI Onsets With Negative Bay in *AL*

[36] In this study we treated auroral onsets that occur near the poleward edge of the auroral oval and are associated with a sharp decrease in *AL* as probable PBIs. Evidence to support this classification is the lack of LANL/SOPA particle injections and the lack of midlatitude Pi2 pulsations. PBIs are also associated with bursty bulk flows in the plasma sheet [*Lyons et al.*, 1999; *Zesta et al.*, 2002], but no Geotail plasma data are available for any of the PBIs in this study. However, all events display a sharp decrease in the local *AL* index that exceeds −50 nT and show some poleward expansion of the auroral oval, which are similar to features observed in substorm auroral onsets. All the PBIs observed could be classified as east-west arcs as discussed by *Zesta et al.* [2002]. Of the seven PBIs identified, five had an HD present in the EICs and three of those had a simultaneous EIC vortex. Two of the PBIs did not have an HD associated with them. Of the five events with a HD, the HD was equatorward of the PBI onsets in four of the five cases. Since PBIs are expected to occur near the poleward boundary of the auroral oval the fact that one PBI occurs equatorward of the HD suggests that we may have misidentified the auroral onset. However, the conflicting observations suggest that this single event is ambiguous and should be excluded from the bulk of the substorm auroral onsets. With the five events that show a HD we calculated the mean difference between the PBI auroral onset and the HD is −0.6° with the PBI onset poleward of the HD. This value is surprisingly similar to the difference between the substorm auroral onset and the HD.

[37] On the basis of observation of negative enhancements in the X component of ground magnetometer data recorded near PBI onsets observed by *Lyons et al.* [1999] and *Rostoker* [2002], we would expect that the PBIs would be most likely to occur within the WEJ. With the limited number of events observed we found that five PBI onsets out of seven occurred within the WEJ and two occurred within the EEJ. *Zesta et al.* [2002] demonstrated for their 12 east-west PBI events that the bulk of the distribution occurred between 19 and 24 MLT. Our PBI onset had a mean location of 23.9 MLT. This range also encompassed the mean location of the substorm auroral onsets, which is 23 MLT [*Frey et al.*, 2004; *Frey and Mende*, 2006] and HD. Since the PBIs and HDs occur at about the same mean location it would not be unreasonable to find that the PBI could occur within either the eastward electrojet or the westward electrojet. Similar observations of substorm auroral onsets within the EEJ were found in this study as well.

5.3. Substorm Onset With Negative Bay in *AL* and a Harang Discontinuity

[38] Twenty-six of the 58 remaining substorm onsets had a sharp drop in the *AL* index and occurred nearly simultaneously with a HD during the growth phase and 28 had a sharp drop and a HD during the expansion phase. The mean difference in latitude between the onset location and the HD

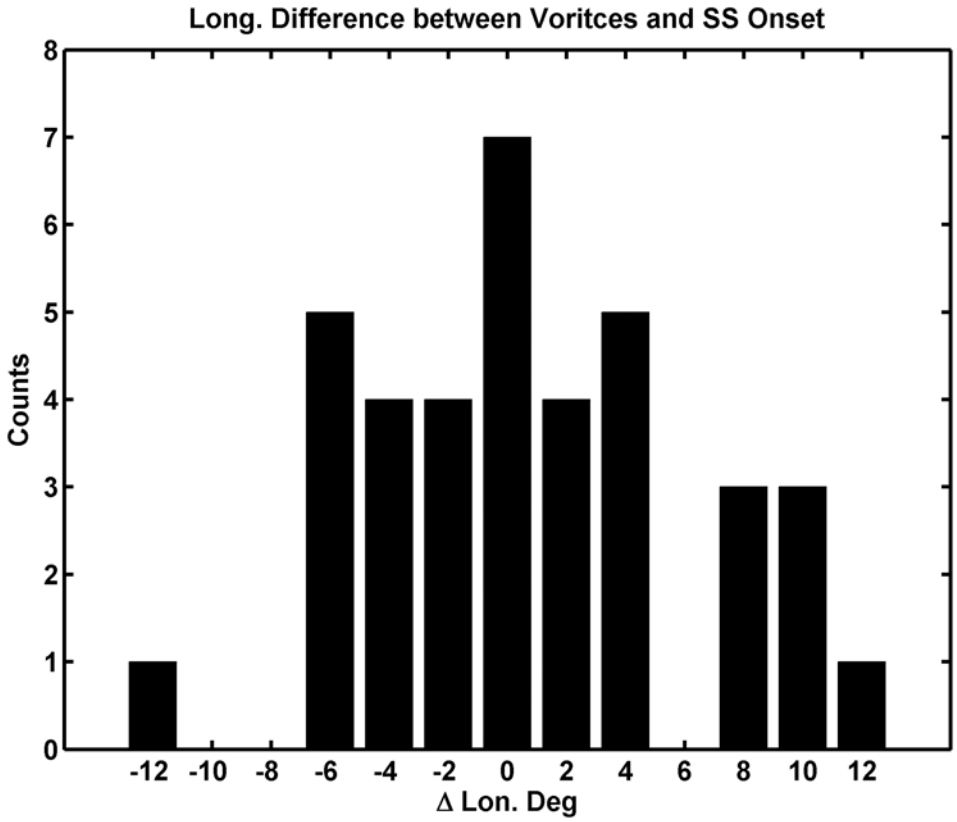

Figure 11. Histogram of the difference in longitude between the substorm onset and the equivalent ionospheric current vortex during the expansion phase. Negative values indicate that the vortex is to the west of the onset position and positive values for vortices to the east.

during the growth phase and the expansion phase is consistent with *Nielsen and Greenwald* [1979] who found using STARE radar data that the onsets are located poleward of the HD. However, Nielsen and Greenwald also noted that some of their onsets were located equatorward of the HD, which corresponds to our onsets that occurred within the eastward electrojet.

[39] The bulk of our observations do not agree with the results reported by *Baumjohann et al.* [1981] and *Koskinen and Pulkkinen* [1995]. These authors concluded that the onset generally occurs slightly equatorward of the HD as identified with the STARE radar data. Our results are not completely inconsistent, however, because *Kamide and Vickrey* [1983] found the HD defined by the reversal of the north-south electric field is located 1° to 2° poleward of the discontinuity identified by ground magnetic perturbations. If we take our difference in location into account, then the bulk of our observation lie within the HD with some onsets occurring equatorward of the HD as observed in the radar data by *Baumjohann et al.* [1981] and *Koskinen and Pulkkinen* [1995] but more onsets occurring poleward of the HD as recorded by *Nielsen and Greenwald* [1979]. However, the location of the two HDs is reversed in the work of *Amm* [2003], which would put many of our onset observations equatorward of the HD determined from the STARE radar.

[40] Ideally, to better relate our results to the previous radar and ground magnetometer studies, we need a number of simultaneous images of substorm onsets and observations of the HD identified in both the radar data and the ionospheric equivalent currents. Fortunately, 2 of our 75 onset events have the HD identified with both methods. Figure 12 displays the equivalent ionospheric currents (green vectors) and the STARE radar electric field data (blue vectors) on 27 January 2003 at 2307 UT. The long red bar marks the HD visible in the equivalent ionospheric current data, which we will refer to as EICHD, and the short red bar marks the HD visible in the electric field data, which we will refer to as the EHD. The red asterisk indicates the position of the onset as identified from the IMAGE auroral image. If we assume that the EHD extends further to the west, then it appears that the substorm onset occurs between the locations of the HD as defined by the two methods. We can draw the same conclusion from an examination of another event on 8 March 2003 at 2142 UT (not shown). We can also see in Figure 12 that the approximate latitudinal difference in the two HDs is about 2°, consistent with the work of *Kamide and Vickrey* [1983] and *Kunkel et al.* [1986]. The difference in latitude for the March 8, 2003 event is about 2.5° and not that different from Kamide and Vickrey and similar to the 2° to 3° difference observed by *Kunkel et al.* [1986]. This difference is similar to that of *Amm* [2003], however, Amm et al. found the magnetic convection reversal boundary poleward of the ionospheric plasma convection reversal boundary for observations taken at about 0300 MLT and in a similar location to the HDs shown in

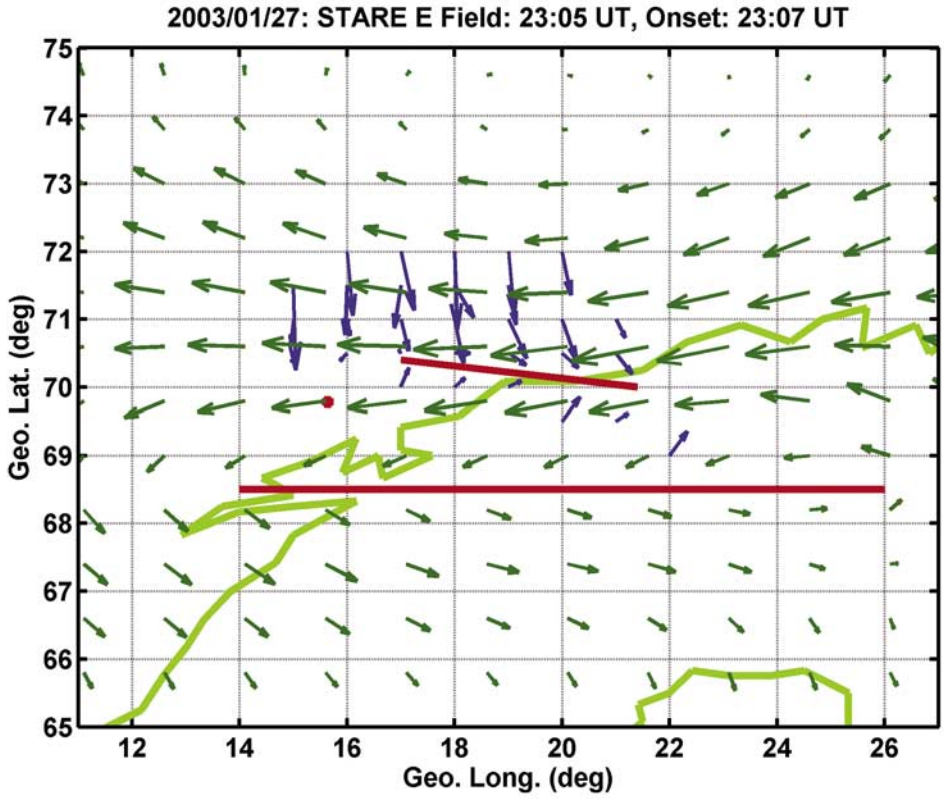

Figure 12. Near simultaneous equivalent ionospheric currents and STARE electric field data for 27 January 2003. The green vectors represent the equivalent ionospheric currents, blue vectors are the STARE electric field data, and the light green curve is the outline of Scandinavia. The red segment at 68.5° geographic latitude is the HD identified in the equivalent ionospheric currents. The red segment at about 70° geographic latitude is the possible HD in the STARE electric field data and the red asterisk 15.6° geographic longitude and 69.8° geographic latitude is the substorm onset location.

Figure 12. Amm et al. believe this difference in location is due to the positive gradient of the absolute value of the field aligned current in the postmidnight sector. A location of the onset between the two HDs is consistent with observations in our study, the *Baumjohann et al.* [1981] and the *Koskinen and Pulkkinen* [1995] work, and is consistent with the few substorm onsets that occurred equatorward of the HD in the work of *Nielsen and Greenwald* [1979].

[41] The observations of an onset equatorward of the EHD raise an interesting point. If the EHD and the EICHD are actually colocated as suggested by *Kamide and Vickrey* [1983] but not observed in the work of *Kunkel et al.* [1986] and *Amm* [2003] and appear offset in the measurements, then onsets equatorward of the EHD would place them in the EEJ. This location is contradictory to the idea that substorm onsets occur in the WEJ. The solution to this difference is not clear at this time and more simultaneous events should be examined.

[42] Another important feature that is apparent in Figure 12 is the angle between the electric field vectors and the equivalent ionospheric currents. Ideally, we expect the two different vectors to be perpendicular to one another when the ionospheric conductances are uniform, which is most likely not the case during substorms. The two different vectors, however, are nearly perpendicular to one another in Figure 12. A similar observation was made by *André and Baumjohann* [1982] and they concluded that little or no conductivity gradient was present in the ionosphere. The fact that these two vectors in our study from two independent measurements are nearly perpendicular to one another supports the reliability of the equivalent ionospheric currents even if we do not know the details of the ionospheric conductivity.

[43] *Lyons et al.* [2003] stated that they expect all substorm onsets to be located within the HD near the upward FAC. However, we find only 40% of substorm onsets support this expectation during the growth phase and about half of the onsets support this expectation during the expansion phase. Events that do not meet the criteria of this category will be discussed in a following section. Only 18 HDs are continuously present throughout the growth phase, onset, and the expansion phase. Nevertheless, it is unclear whether the HDs are expected to be continuously present throughout the growth phase, onset, and expansion phase. Table 1, Figure 4, and Figure 5 show that even for the events in which a HD was present the onset location is not exactly within the equivalent ionospheric current HD during the growth phase and only three onsets are within it during the expansion phase. In this study, the phrase "exactly within the equivalent ionospheric current HD"

means that within the resolution of the equivalent ionospheric currents the onset occurs in the region between the EEJ and the WEJ where we believe that $J_y = 0$ in geographic coordinates has most likely occurred. However, during both the growth phase and the expansion phase the bulk of the onsets were within the EIC WEJ as is expected [*Rostoker*, 1996]. Not expected is the fact that a few onsets were observed within the EIC EEJ. Observations of onsets outside of the HD raise the question: how far do the onsets need to be from the HD to be no longer considered colocated? A more detailed analysis of the equivalent ionospheric currents is required to more accurately answer this question. In the next two sections we will examine the two other categories and demonstrate the range of equivalent ionospheric current structures and onset locations.

5.4. Substorm Onset With Negative Bay in *AL* and Vortices

[44] Many of the substorms showed a vortex in the equivalent ionospheric currents during the growth phase and even more displayed a vortex during the expansion phase. Many of these vortices were counterclockwise and generally located equatorward of the substorm onset. A number of clockwise vortices were observed as well and the majority of these were poleward in the polar cap region. Several studies have reported a nearly simultaneous association between equivalent ionospheric current vortices and substorms onsets [*Untiedt et al.*, 1978; *Küppers et al.*, 1979; *Opgenoorth et al.*, 1980; *André and Baumjohann*, 1982; *Untiedt and Baumjohann*, 1993; *Lyatsky et al.*, 2001] but most of these studies examined only a single event. *Untiedt et al.* [1978] describe a counter clockwise vortex in equivalent ionospheric current before the substorm onset and this vortex was colocated with an auroral spiral having the same rotation. Unfortunately, the resolution of the IMAGE auroral imager is not sufficient for us to determine the details of the discrete aurora during our observations of the current vortices. Table 1 shows that there are 20 more vortices present during the expansion phase than during the growth phase. This fact suggests that the substorm current wedge influences the formation of the vortices. However, in 17 of the onsets the vortex was already present before the auroral onset time, as was the case in the *Untiedt et al.* [1978] study, and the vortex occurred before the onset time observed in the local *AL* index. This result suggests that the substorm onset is associated with a region of outward field-aligned current present prior to the auroral brightening. Observations of equivalent ionospheric current vortices have also been made during traveling convection vortices [*Lyatsky et al.*, 1999a, 1999b; *Moretto et al.*, 2002] and associated with omega bands [*André and Baumjohann*, 1982]. They have been also observed in the region of the HD during intervals without substorms [*Pulkkinen et al.*, 2003]. We also investigated whether the vortices are the result of general auroral electrojet activity and found that nine of the vortices observed before the auroral electrojet onset and auroral image onset occurred during quiet conditions when the local *AE* is less than 100 nT and the other 12 occur during more active intervals.

[45] *Opgenoorth et al.* [1980] also observed a counterclockwise vortex poleward of the auroral oval before the substorm and a clockwise vortex poleward for 3 min afterward, but these vortices were observed in the differential currents. As far as we are aware, a vortex was not directly observed in the equivalent ionospheric currents. Furthermore, a quantitative value for the separation between the onset location and the center of the vortex was not given. This study also noted that a counter clockwise rotation of the currents should occur around an upward field-aligned current (FAC) and a downward FAC would occur at a clockwise spiral in the currents only for uniform ionospheric conductances.

[46] The large review of polar current systems by *Untiedt and Baumjohann* [1993] discusses many aspects of the HD and vortices that are beyond the scope of this paper. One important aspect they note upon interpreting the vortex observed in the work of *Küppers et al.* [1979] is that the HD may upon occasion consist of a series of counter clockwise equivalent ionospheric current vortices. See Figure 40 of *Untiedt and Baumjohann* [1993]. This interpretation is similar to our observations in our category of simultaneous HDs and vortices; however, we generally see only one vortex embedded within the HD. See our Figure 7. Furthermore, Table 1 indicates that a simultaneous HD and vortex is not frequently observed, but we have recorded it about 10% of the time.

[47] The study of *Lyatsky et al.* [2001] reported a near simultaneous equivalent ionospheric current vortex during a substorm. In their study a substorm began about 0330 UT on 2 March 1997 and shortly afterward at 0337 UT a clockwise vortex occurred in the equivalent ionospheric currents and lasted for over 3 h. A counterclockwise vortex was also observed later at about 0345 UT and this vortex lasted for over an hour. Whether the two vortices were simultaneously present during the onset could not be determined due to the limited equatorward extent of the available magnetometer data. From 0410 UT to 0432 UT, Interball auroral UV images were available and displayed a double oval structure that was limited in local time and auroral bubbles or petals were attached to a bright protuberant region at the equatorward boundary of the auroral oval. No vortices or spirals, however, were observed in the aurora and a quantitative measure for the separation between the vortices centers and the substorm onset location was not possible.

[48] The previous studies that report an equivalent ionospheric current vortex around the time of a substorm do not give a quantitative difference in latitude and longitude between the onset location and the vortex location. In our study we found that the mean difference in latitude is less than a degree and the mean difference in longitude is about 1.5° for the vortices observed during both the growth and expansion phase. However, this erroneously suggests that the aurora onset is nearly colocated with an equivalent ionospheric current vortex. Figure 8 and Figure 9 show a wide distribution with a standard deviation of about 3° in latitude during both the growth and expansion phase. Furthermore, these figures appear to have two peaks. This is expected because both clockwise vortices, which normally appear at the same latitude or equatorward of the onset location, and counterclockwise vortices, which always appear poleward of the onset location, have been included in the plots. The different types of vortices have not been separated due to the limited number of events in the

distribution. The significant standard deviation of the distribution indicates, however, that the vortices occur over a range of latitudes.

[49] The broad distribution of the longitudinal differences between the equivalent ionospheric current vortices and the onsets shown in Figures 10 and 11 demonstrates the large range of differences in longitude. The widths of the longitudinal distributions are influenced by the onset auroral arc. The longitude of the onset is more difficult to determine than the latitude because an auroral arc brightens over some length and not just a point. However, at the latitude of the auroral oval 1° degree of latitude equates to about 110 km, while 1° degree of longitude is only about 50 km. This means that the standard deviation of these two longitudinal distributions for the vortices, which is about 5.6° in longitude, has about the same length in kilometers (i.e., about 280 km) as the standard deviation of the latitudinal distributions. However, we interpret the large standard deviation of the distributions in Figures 10 and 11 to mean that there is no clear one to one correlation between the EIC vortices and the auroral onset location. Furthermore, these distributions also show that there is no preference in the longitudinal direction for the clockwise or counterclockwise vortices.

[50] Similar to the onsets occurring near the HD, the bulk of the onsets in this category occur in the EIC WEJ, which is consistent with *Rostoker* [1996]. See Table 1. During the growth phase 16 of 17 onsets are within the EIC WEJ and 33 of 37 onsets during the expansion phase. Only a small fraction of the onsets during both phases occurred within the EIC EEJ and both of these onsets were within a degree of the EIC WEJ.

5.5. Substorm Onsets With a Negative Bay in *AL* and No Harang Discontinuity

[51] Of the initial 75 onsets one third exhibit a sharp decrease in the *AL* index but no simultaneous HD or vortex during the growth phase. During the expansion phase even fewer onsets had a sharp decrease in the *AL* index and no simultaneous HD or vortex. Examination of these onsets indicates that many of them occurred in either the pre-HD sector or the post-HD sector. Figure 1 shows that within the pre-HD and post-HD sectors there is a shear between an eastward electrojet and weaker westward polar cap ionospheric current as well as westward electrojet and weaker eastward subauroral return current; hence, this could be interpreted as a HD. However, this shear in the currents is not the classical Harang shear discussed in the work of *Maynard* [1974] and *Heppner* [1977] and these events are not considered in the HD statistics. The pre-HD and post-HD sectors can be identified by examining the magnitude of the currents. The currents within the auroral oval electrojet are considerably larger than those poleward or equatorward of the auroral oval. Figure 1 also indicates this difference in magnitude. For example, in Figures 3 and 7 the EICs at the lowest latitudes of the figures have a smaller magnitude than those to the east and west of the HD. These smaller magnitude currents would be equatorward of the auroral oval. Similar observations are apparent for the EICs poleward of the auroral oval. A shear between a weak poleward westward EIC and a strong equatorward eastward EIC would most likely be a premidnight shear. A shear between a weak poleward eastward EIC and a strong equatorward westward EIC would most likely be a premidnight shear.

[52] In a separate subcategory we were unable to determine where the onset occurred with respect to the HD. The pattern of the equivalent ionospheric currents associated with these onsets in this subcategory is difficult to relate to the general picture given in Figure 1 because of the complex nature of the currents during both the growth phase and expansion phase.

[53] The final subcategory we consider here is a subset of onsets that occur in a unidirectional current that is either EIC WEJ or EIC EEJ over the entire two dimensional array of equivalent ionospheric currents. No HDs or vortices are observed in these events. The onsets that occur in the unidirectional equivalent ionospheric current are interesting because they do not match any previous observations nor do they satisfy the *Lyons et al.* [2003] statement that all onsets should occur within the HD. It is quite possible that the HD is located further equatorward for the onsets within the EIC WEJ or located further poleward for the onsets within the EIC EEJ. However, even if this is the case the onset is still about 7° in latitude or more away from the HD and it suggests that the auroral oval is quite wide. Even more interesting are those events that occur within mainly the EIC EEJ. Not only do these events disagree with *Lyons et al.* [2003], but they are also inconsistent with the general idea that substorm onset occurs within the westward electrojet [*Rostoker*, 1996].

[54] For as many events as possible we examined the IMAGE auroral images to further verify the onset observations. An examination of the available auroral images shows that three of the events occur during periods when IMAGE observes the auroral oval at a large angle with respect to zenith at the position of the initial brightening. We believe this near edge-on observation of the midnight sector of the auroral oval would make it difficult to accurately identify the position of the auroral oval. However, unless the locations of the onsets are off by over 7° in latitude or over 13° in longitude, which is the half width of the two dimensional array of equivalent currents, the equivalent ionospheric currents still do not show a HD near the onset.

6. Summary and Conclusions

[55] In this study we examined 75 cases of auroral onset identified by the IMAGE FUV imager that occurred almost directly over the IMAGE ground magnetometer array. We determined that 10 of the ''onsets'' looked more like pseudo breakups and 7 appeared to be more like PBIs than substorm expansions so these were not considered further in our study. Of the remaining 58 onsets, 40% occurred on average about 1° poleward of the HD identified with the equivalent ionospheric currents during the growth phase of the substorm and about half occurred on average about 1° poleward of the HD during the expansion phase. The location of these onsets with respect to the HD supports most of the previous studies on near simultaneous substorm onsets and the HD. Of the 26 HDs present during the growth phase only 18 were continuously present during the growth phase, onset, and expansion phase. In two onsets both equivalent ionospheric currents and STARE radar data are available and these data indicated that the auroral onset

occurred in between the HDs identified in the separate data sets. The HDs identified in the radar data are located about 1° to 3° poleward of the HDs shown in the equivalent ionospheric current data. However, 35 onsets did not appear to occur near the classical HD observed during the growth phase. During the expansion phase 51% of the onsets did not appear to occur near the classical HD. In both phases of the substorm some onsets did not occur in the equivalent ionospheric westward electrojet. We have also observed that 29% of the substorm onsets occur near both equivalent ionospheric current clockwise and counter clockwise vortices observed during the growth phase and about twice as many of the substorm onsets occur near both vortices during the expansion phase. These vortices have been observed in previous studies, but this study provides the first simple statistical breakdown on the frequency of occurrence and distribution of their location. In four categories nearly all the onsets appear to be associated with the EIC WEJ and some occurred within the HD. This observation is to be expected, but a few onsets occurred within the EIC EEJ, which contradicts the present concept that the location of substorm onset should be within the westward electrojet.

[56] The results of this study demonstrate that substorm onset does not always occur near the HD and the relationship between the substorm onset and the HD is not simple. Furthermore, we have also shown that even when substorms are well identified in the auroral images the expected simultaneous particle injection at geosynchronous orbit and sharp drop in the local *AL* index are not always present even when the onset appears to occur in close proximity to the detectors.

[57] **Acknowledgments.** This work was supported by NASA grant NNG05GE00G.We would like to thank S. Mende for providing the IMAGE auroral images to the NSSDC and thank NSSDC for making those images available to the community. We thank the institutes who maintain the IMAGE magnetometer array especially the PI institution: the Finnish Meteorological Institute. We thank E. Zesta and V. Angelopoulos for many useful discussions. We would also like to thank M.G. Henderson for providing the LANL/SOPA plots and L.L. Lyons for his advice while doing this study. UCLA Institute of Geophysics and Planetary Physics Publication 6346.

[58] Wolfgang Baumjohann thanks Gordon Rostoker and another reviewer for their assistance in evaluating this paper.

References

Akasofu, S.-I. (1964), The development of the auroral substorm, *Planet. Space Sci.*, *12*, 273–282, doi:10.1016/0032-0633(64)90151-5.

Amm, O. (1997), Ionospheric elementary current systems in spherical coordinates and their application, *J. Geomagn. Geoelectr.*, *49*, 947–955.

Amm, O. (1998), Method of characteristics in spherical geometry applied to a Harang discontinuity situation, *Ann. Geophys.*, *16*, 413–424, doi:10.1007/s00585-998-0413-2.

Amm, O., and A. Viljanen (1999), Ionospheric disturbance magnetic field continuation from the ground to the ionosphere using spherical elementary current systems, *Earth Planets Space*, *51*, 431–440.

Amm, O., P. Janhunen, H. J. Opgenoorth, T. I. Pulkkinen, and A. Viljanen (2000), Ionospheric shear flow situations observed by the MIRACLE network and the concept of Harang discontinuity, in *Magnetospheric Current Systems*, *Geophys. Monogr. Ser.*, vol. 118, edited by S. Ohtani et al., p. 227, AGU, Washington, D. C.

Amm, O., et al. (2003), Mesoscale structure of a morning sector ionospheric shear flow region determined by conjugate Cluster II and MIRACLE ground-based observations, *Ann. Geophys.*, *21*, 1737–1751.

André, D., and W. Baumjohann (1982), Joint two-dimensional observations of ground magnetic and ionospheric electric fields associated with auroral currents 5. Current systems associated with eastward drifting omega bands, *J. Geophys.*, *50*, 194–201.

Baumjohann, W., R. J. Pellinen, H. J. Opgenoorth, and E. Nielsen (1981), Joint two-dimensional observations of ground magnetic field and ionospheric electric fields associated with auroral zone currents: current systems associated with local auroral break-ups, *Planet. Space Sci.*, *29*, 431–447, doi:10.1016/0032-0633(81)90087-8.

Burch, J. L. (2003), The first two years of IMAGE, *Space Sci. Rev.*, *109*, 1–24, doi:10.1023/B:SPAC.0000007510.32068.68.

Erickson, G. M., R. W. Spiro, and R. A. Wolf (1991), The physics of the Harang discontinuity, *J. Geophys. Res.*, *96*, 1633–1645, doi:10.1029/90JA02344.

Fairfield, D. H., and G. D. Mead (1975), Magnetospheric mapping with a quantitative geomagnetic field model, *J. Geophys. Res.*, *80*, 535–542, doi:10.1029/JA080i004p00535.

Frey, H. U., and S. B. Mende (2006), Substorm onsets as observed by IMAGE-FUV, in *Substorms VIII: Proceedings of ICS-8*, pp. 71–75, edited by M. Syrjasuo and E. Donovan, Univ. of Calgary Press, Calgary, Ontario, Canada.

Frey, H. U., S. B. Mende, V. Angelopoulos, and E. F. Donovan (2004), Substorm onset observations by IMAGE-FUV, *J. Geophys. Res.*, *109*, A10304, doi:10.1029/2004JA010607.

Harang, L. (1946), The mean field of disturbance of polar geomagnetic storms, *Terr. Magn. Atmos. Electr.*, *51*, 353–380, doi:10.1029/TE051i003p00353.

Heppner, J. P. (1972), The Harang discontinuity in auroral belt ionospheric currents, *Geophys. Norv.*, *29*, 105–120.

Heppner, J. P. (1977), Empirical models of high-latitude electric fields, *J. Geophys. Res.*, *82*, 1115–1125, doi:10.1029/JA082i007p01115.

Kamide, K. (1978), On current continuity at the Harang discontinuity, *Planet. Space Sci.*, *26*, 237–244, doi:10.1016/0032-0633(78)90089-2.

Kamide, K., and J. F. Vickrey (1983), Variability of the Harang discontinuity as observed by the Chatanika RADAR and the IMS Alaska magnetometer chain, *Geophys. Res. Lett.*, *10*, 159–162, doi:10.1029/GL010i002p00159.

Kauristie, K., T. I. Pulkkinen, R. J. Pellinen, and H. J. Opgenoorth (1996), What can we tell about global auroral-electrojet activity from a single meridional magnetometer chain?, *Ann. Geophys.*, *14*, 1177–1185, doi:10.1007/s005850050380.

Koskinen, H. E. J., and T. I. Pulkkinen (1995), Midnight velocity shear zone and the concept of Harang discontinuity, *J. Geophys. Res.*, *100*, 9539–9547, doi:10.1029/95JA00228.

Koskinen, H. E. J., R. E. Lopez, R. J. Pellinen, T. I. Pulkkinen, D. N. Baker, and T. Bsinger (1993), Pseudo breakup and substorm growth phase in the ionosphere and magnetosphere, *J. Geophys. Res.*, *98*, 5801–5813, doi:10.1029/92JA02482.

Kunkel, T., W. Baumjohann, J. Untiedt, and R. A. Greenwaldt (1986), Electric fields and currents at the Harang discontinuity: A case study, *J. Geophys.*, *59*, 73–86.

Küppers, F., J. Untiedt, W. Baumjohann, K. Lange, and A. G. Jones (1979), A two-dimensional magnetometer array for ground-based observations of auroral zone electric currents during the international magnetospheric study (IMS), *J. Geophys.*, *46*, 429–450.

Lyatsky, W. B., G. J. Sofko, A. V. Kustov, D. André, W. J. Hughes, and D. Murr (1999a), Traveling convection vortices as seen by the SuperDARN HF radars, *J. Geophys. Res.*, *104*, 2591–2601, doi:10.1029/1998JA900007.

Lyatsky, W. B., A. V. Kustov, G. J. Sofko, B. Jacobsen, D. André, and L. L. Cogger (1999b), Ionospheric convection and equivalent ionospheric currents in the dayside high-latitude winter ionosphere, *J. Geophys. Res.*, *104*, 22,525–22,533, doi:10.1029/1999JA900266.

Lyatsky, W., L. L. Cogger, B. Jackel, A. M. Hamza, W. J. Hughes, D. Murr, and O. Rasmussen (2001), Substorm development as observed by Interball UV imager and 2-D magnetic array, *J. Atmos. Sol. Terr. Phys.*, *63*, 1609–1621, doi:10.1016/S1364-6826(01)00045-1.

Lyons, L. R., T. Nagai, G. T. Blanchard, J. C. Samson, T. Yamamoto, T. Mukai, A. Nishida, and S. Kokubun (1999), Association between Geotail plasma flow and auaoral poleward boundary intensifications observed by CANOPUS photometers, *J. Geophys. Res.*, *104*, 4485–4500, doi:10.1029/1998JA900140.

Lyons, L. R., C.-P. Wang, and T. Nagai (2003), Substorm onset by plasma sheet divergence, *J. Geophys. Res.*, *108*(A12), 1427, doi:10.1029/2003JA010178.

Maynard, N. C. (1974), Electric field measurements across the Harang discontinuity, *J. Geophys. Res.*, *79*, 4620–4631, doi:10.1029/JA079i031p04620.

Mende, S. B., H. U. Frey, T. J. Immel, J.-C. Gerard, B. Hubbert, and S. A. Fuselier (2003), Global imaging of proton and electron aurorae in the far ultraviolet, *Space Sci. Rev.*, *109*, 211–254, doi:10.1023/B:SPAC.0000007520.23689.08.

Moretto, T., M. Hesse, A. Yahnin, A. Ieda, D. Murr, and J. F. Watermann (2002), Magnetospheric signature of an ionospheric traveling convection vortex event, *J. Geophys. Res.*, *107*(A6), 1072, doi:10.1029/2001JA000049.

Nakamura, R., D. N. Baker, T. Yamamoto, R. D. Belian, E. A. Bering, J. A. Benbrook, and J. R. Theal (1994), Particle and field signatures during pseudobreakup and major expansion onset, *J. Geophys. Res.*, *99*, 207–221, doi:10.1029/93JA02207.

Nielsen, N. E., and R. A. Greenwald (1979), Electron flow and visual aurora at the Harang discontinuity, *J. Geophys. Res.*, *84*, 4189–4200, doi:10.1029/JA084iA08p04189.

Opgenoorth, H. J., R. J. Pellinen, H. Maurer, F. Küppers, W. J. Heikkila, and P. Tanskanen (1980), Ground-based observations of an onset of localized field-aligned currents during auroral breakup around magnetic midnight, *J. Geophys.*, *48*, 101–115.

Pulkkinen, T. I., D. N. Baker, M. Wiltberger, C. Goodrich, R. E. Lopez, and G. Lyon (1998), Pseudobreakup and substorm onset: Observations and MHD simulations compared, *J. Geophys. Res.*, *103*, 14,847–14,854, doi:10.1029/97JA03244.

Pulkkinen, A., O. Amm, and A. Viljanen (2003), Ionospheric equivalent current distributions determined with the method of spherical elementary current systems, *J. Geophys. Res.*, *108*(A2), 1053, doi:10.1029/2001JA005085.

Rostoker, G. (1996), Phenomenology and physics of magnetospheric substorms, *J. Geophys. Res.*, *101*, 12,955–12,973, doi:10.1029/96JA00127.

Rostoker, G. (2002), Identification of substorm expansive phase onsets, *J. Geophys. Res.*, *107*(A7), 1137, doi:10.1029/2001JA003504.

Untiedt, J., and W. Baumjohann (1993), Studies of polar current systems using the IMS Scandinavian magnetometer array, *Space Sci. Rev.*, *63*, 245–390, doi:10.1007/BF00750770.

Untiedt, J., R. Pellinen, F. Küppers, H. J. Opgenoorth, W. D. Pelster, W. Baumjohann, H. Ranta, J. Kangas, P. Czechowsky, and W. J. Heikkila (1978), Observations of the initial development of an auroral and magnetic substorm at magnetic midnight, *J. Geophys.*, *45*, 41–56.

Zesta, E., E. Donovan, L. Lyons, G. Enno, J. S. Murphree, and L. Cogger (2002), Two-dimensional structure of auroral poleward boundary intensifications, *J. Geophys. Res.*, *107*(A11), 1350, doi:10.1029/2001JA000260.

O. Amm, K. Kauristie, A. Koistinen, and A. Viljanen, Space Physics Program, Meteorological Institute, Vuorikatu 15A, P. O. Box 503, FIN-00101 Helsinki, Finland.

H. U. Frey, Space Sciences Laboratory, University of California, Berkeley, Grizzly Peak at Centennial Drive, Berkeley, CA 94720-7450, USA.

R. L. McPherron and J. M. Weygand, Institute of Geophysics and Planetary Physics, University of California, Los Angeles, 3845 Slichter Hall, P. O. Box 951567, Los Angeles, CA 90095, USA. (jweygand@igpp.ucla.edu)